Article:
Bull, K, Hallam, A, Papić, Z et al. (1 more author) (2022) Tuning between continuous time crystals and many-body scars in long-range XYZ spin chains. Physical Review Letters, 129 (14). 140602. ISSN 0031-9007

https://doi.org/10.1103/PhysRevLett.129.140602

Tuning between Continuous Time Crystals and Many-Body Scars in Long-Range *XYZ* Spin Chains

Kieran Bull,[1] Andrew Hallam,[1] Zlatko Papić,[1] and Ivar Martin[2]
[1]*School of Physics and Astronomy, University of Leeds, Leeds LS2 9JT, United Kingdom*
[2]*Material Science Division, Argonne National Laboratory, Argonne, Illinois 08540, USA*

(Received 10 May 2022; accepted 18 August 2022; published 29 September 2022)

Persistent oscillatory dynamics in nonequilibrium many-body systems is a tantalizing manifestation of ergodicity breakdown that continues to attract much attention. Recent works have focused on two classes of such systems: discrete time crystals and quantum many-body scars (QMBS). While both systems host oscillatory dynamics, its origin is expected to be fundamentally different: discrete time crystal is a phase of matter which spontaneously breaks the $\mathbb{Z}_2$ symmetry of the external periodic drive, while QMBS span a subspace of nonthermalizing eigenstates forming an su(2) algebra representation. Here, we ask a basic question: is there a physical system that allows us to tune between these two dynamical phenomena? In contrast to much previous work, we investigate the possibility of a *continuous* time crystal (CTC) in undriven, energy-conserving systems exhibiting prethermalization. We introduce a long-range *XYZ* spin model and show that it encompasses both a CTC phase as well as QMBS. We map out the dynamical phase diagram using numerical simulations based on exact diagonalization and time-dependent variational principle in the thermodynamic limit. We identify a regime where QMBS and CTC order coexist, and we discuss experimental protocols that reveal their similarities as well as key differences.

DOI: 10.1103/PhysRevLett.129.140602

Introduction.—The basic tenet of thermodynamics is that when a substance contains many constituents, its macroscopic behavior can be efficiently described by just a few variables such as pressure, volume, and temperature. Microscopic details typically only enter through the mechanism of dissipation, which accounts for the energy transfer from the large to the microscopic scale (heating). Generally, the higher the temperature the faster the relaxation of any nongeneric state that possesses some ordering, such as magnetization, unless the latter is explicitly conserved by the system's Hamiltonian.

It therefore came as a surprise when Rydberg atom experiments [1] revealed long-lived oscillations of an order parameter in a very high energy density initial state. The oscillations were subsequently understood to be due to quantum many-body scars (QMBSs): a dynamically decoupled subspace, spanned by nonthermalizing many body eigenstates, which is not protected by any symmetry [2,3]. This system evades rapid relaxation due to the fact that QMBS eigenstates form "towers" with (nearly) equidistant energy spacing. Superpositions of tower states undergo periodic evolution, therefore avoiding the dephasing that afflicts generic states. These QMBS towers can be understood semiclassically [4–8], based on an analogy with quantum scars of a single particle in a stadium billiard [9]. Importantly, this behavior was shown to occur also in higher dimensions [10–12] and in the presence of certain kinds of perturbations [13–15] including disorder [16]. More generally, QMBS subspaces are now understood to originate from a (restricted) spectrum generating algebra [17–19], which has been shown to arise in a number of nonintegrable lattice models [17,20–29]. As the models are nonintegrable, this represents a *weak* violation of the eigenstate thermalization hypothesis (ETH) [30,31].

A seemingly distinct way of evading the ETH is the formation of a continuous time crystal (CTC) [32]. In the CTC phase, the system is in a prethermal state that corresponds to a near-ground state in the rotating frame, while being at a very high energy density in the lab frame [33]. Being at a low temperature in the rotating frame, the system has the possibility to develop an order parameter, spontaneously breaking a symmetry which may be unique to the rotating frame. Eventually, the system is expected to fully thermalize; however, if both the prethermalization timescale and the thermalization timescale (corresponding to full equilibration in the lab frame) increase with the system size, the result would be a long-lived, quasistatic ordering in the rotating frame, manifesting as a "rotating" order parameter in the lab frame.

In this Letter, we address the following question: are CTC and QMBS distinct mechanisms of ETH breaking? The two *a priori* appear different: QMBSs reveal themselves for very special initial states, while CTC, being a phase of matter, is supposed to be characterized by an order parameter, with the same order parameter configuration (defined down to physically small but microscopically large volume) possibly originating from very

different microscopic states. Nevertheless, one might wonder if underlying the CTC there are scarlike towers of states that violate the ETH. Below we introduce a long-range XYZ spin model, experimentally motivated by systems of trapped ions and polar molecules, which realizes *both* QMBS as well as CTC route for evading the ETH. For sufficiently long-range interactions, our simulations using infinite matrix product state methods reveal signatures of spontaneous symmetry breaking in the thermodynamic limit and the formation of CTC. For weakly anisotropic couplings and irrespective of interaction range, we demonstrate the existence of QMBS. While the phase diagram contains regimes where CTC and QMBS coexist, we argue that they are distinct phenomena and we discuss experimental protocols that can distinguish between them.

The model and its phase diagram.—Recent experiments [34–39] have realized discrete time crystals (DTC), which dynamically break the $\mathbb{Z}_2$ Ising symmetry of the Floquet drive [40–44] (for recent reviews of DTCs, see Refs. [45–47]). By contrast, here we consider a disorder-free, undriven XYZ spin model, with anisotropic long-range couplings and in the magnetic field along the z-axis, given by the Hamiltonian:

$$H = \frac{1}{\mathcal{N}} \sum_{i>j} \sum_{\nu=x,y,z} \frac{J_\nu}{|i-j|^\alpha} \sigma_i^\nu \sigma_j^\nu + h_z \sum_i \sigma_i^z, \qquad (1)$$

where σ_i^ν are the standard Pauli matrices on site i, and α controls the power-law decay of the interactions. We assume a 1D chain with open boundary conditions and divide the interaction couplings J^ν with the Kac norm, $\mathcal{N}$ [48], which ensures the energy density is intensive.

Before presenting detailed numerical results on the model in Eq. (1), we give their summary in Fig. 1. The dynamical phase diagram is a function of α and two symmetry-breaking parameters: the anisotropy that leads to U(1) symmetry breaking, $J_{\mathrm{U}(1)} \equiv |J_x - J_y|$, and SU(2) symmetry breaking in the rotating frame, $J_{\mathrm{SU}(2)} \equiv |(J_x + J_y)/2 - J_z|$. The field h_z is assumed to be fixed to some large value $h_z \gg J_\nu$, and the remaining dependence on J_ν and α is sketched. We discuss four main regions of this phase diagram, labeled in Fig. 1.

(i) The static prethermal theorem [33] shows that a Hamiltonian of the form $H = H_0 + h_z Z$, with $Z = \sum_j \sigma_j^z$ possessing an integer spectrum, in the limit of large h_z, can be brought into a form $D + V + h_z Z$ through a series of unitary rotations, where D commutes with Z and V is an exponentially small correction in h_z. Thus, for exponentially long times in h_z, the dynamics of our model is governed by an effective prethermal Hamiltonian $H_{\mathrm{eff}} = D + h_z Z$, which has a U(1) symmetry generated by Z. In [48] we explicitly perform the unitary rotation to first order, finding that the correction terms in V contain α via a power-law dependence similar to the original Hamiltonian, with the overall prefactors $J_{\mathrm{U}(1)}^2/h_z$, $J_{\mathrm{U}(1)} J_{\mathrm{SU}(2)}/h_z$. It follows that the prethermal phase is robust, provided $J_{\mathrm{U}(1)}$, $J_{\mathrm{SU}(2)} \ll h_z$. Moreover, for fixed h_z, numerical scans point to weak dependence of the prethermal phase on α [48]. Finally, at first order in $1/h_z$, it follows that the prethermal phase has a stronger dependence on $J_{\mathrm{U}(1)}$ than on $J_{\mathrm{SU}(2)}$. Thus, the prethermal region of the phase diagram roughly takes the shape of an elliptic cylinder, sketched in Fig. 1.

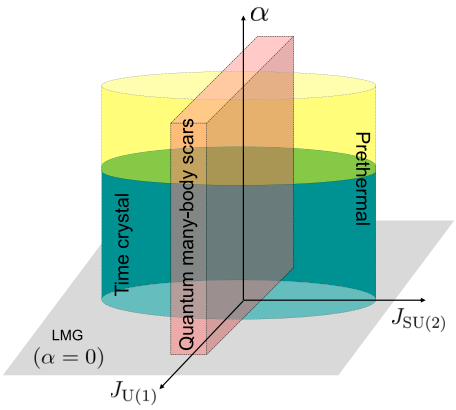

FIG. 1. Schematic summary of the dynamical phase diagram of the model in Eq. (1) as a function of U(1) symmetry breaking $J_{\mathrm{U}(1)}$, SU(2) symmetry breaking $J_{\mathrm{SU}(2)}$ and interaction range α. Within the prethermal regime (yellow), CTC phase emerges for small α and small $J_{\mathrm{U}(1)}$ (green). QMBS (red) are independent of α but require small $J_{\mathrm{SU}(2)}$. The solvable Lipkin-Meshkov-Glick (LMG) limit ($\alpha = 0$) is shown in gray.

(ii) The CTC phase must be a subset of the prethermal region where the emergent U(1) symmetry of the effective Hamiltonian is spontaneously broken. Because of the Mermin-Wagner theorem, in 1D this can only happen if the interactions are sufficiently long-ranged [49,50]. Consistent with this, we observe a transition when $\alpha \sim 2.5$ from a trivial U(1)-preserving phase to a CTC phase. Thus, we expect the prethermal CTC phase to exist within the bounded cylindrical region depicted in Fig. 1.

(iii) The robustness of QMBS is determined by how well the interactions approximately preserve a single tower of Z eigenstates, which is solely dependent on the model's proximity to the isotropic point, $J_x = J_y = J_z$. At this point the model possesses SU(2) symmetry irrespective of α, hence the QMBS region has no α dependence and it is bounded by two planes perpendicular to the $J_{\mathrm{SU}(2)}$ axis. The boundary is sharp as the QMBS behavior diminishes exponentially with $J_{\mathrm{SU}(2)}$ [48].

(iv) Finally, the limit $\alpha = 0$ is a fully connected Lipkin-Meshkov-Glick (LMG) model [51,52], which can be described by only a few collective variables if initial states satisfy permutation symmetry [53–55]. The paramagnetic state ($J_\nu \ll |h_z|$) can be identified with a CTC (Ref. [47] used a term "mean-field time crystal" to distinguish this

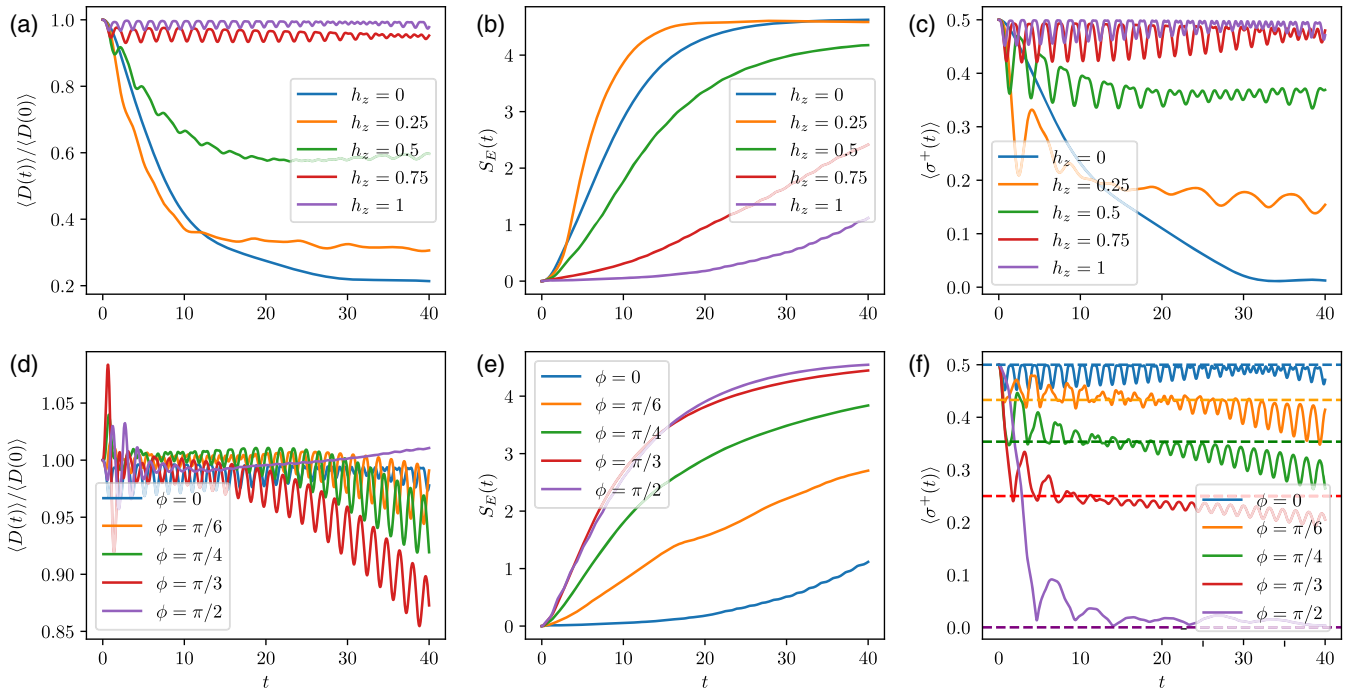

FIG. 2. Signatures of the continuous time crystal. (a) Expectation value of the prethermal Hamiltonian, Eq. (2), in the time evolved state. The value is normalized by its value at time $t = 0$. (b) Order parameter $\langle\sigma^+(t)\rangle$ defined in the text. (c) Entanglement entropy $S_E(t)$. All plots are for the infinite long-range XYZ model in Eq. (1) with $\alpha = 1.13, J_x = -0.4, J_y = -2.0, J_z = -1$. The value of the field h_z is indicated in panels (a)–(c), while $h_z = 1$ in panels (d)–(f). The initial state is given by Eq. (3) with $\phi = 0$ in (a)–(c), and $\phi = \{0, \pi/6, \pi/4, \pi/3, \pi/2\}$ in panels (d)–(f). Dashed lines in (f) denote the average magnetization $\cos(\phi)/2$ after the rapid initial relaxation.

special type of CTC). In the Ising limit, the thermalization time is estimated as $\tau_{\text{th}} \sim N^{\beta/d}$, where $\beta = \min[d - \alpha, (1 + d)/2]$ [56]. Thus for $d = 1$ and $\alpha < 1/2$, thermalization time ($\sim N^{1-\alpha}$) is much longer than prethermalization or order parameter melting time, $\sim N^{1/2}$ [57,58], both diverging with system size.

Numerical evidence for CTC.—For large h_z, sufficiently long-range interactions ($\alpha > d = 1$) and low temperatures, Fig. 2 shows that a prethermal CTC phase emerges in the model given by Eq. (1). Provided h_z is sufficiently large, the dynamics is described—up to a timescale exponential in $h_z/J_{\text{U(1)}}$—by an effective Hamiltonian $H_{\text{eff}} = D + h_z Z$ where D is given by [32]

$$D = \sum_{j>i} \frac{1}{2}(J_x + J_y)\left(\frac{\sigma_i^x \sigma_j^x}{|i-j|^\alpha} + \frac{\sigma_i^y \sigma_j^y}{|i-j|^\alpha}\right) + J_z \frac{\sigma_i^z \sigma_j^z}{|i-j|^\alpha}. \quad (2)$$

This effective Hamiltonian has an emergent U(1) symmetry which is spontaneously broken at low effective temperatures for long-range interactions ($\alpha \lesssim 2.5$) [50]. To avoid the challenges of observing spontaneous symmetry breaking in finite volume, in Fig. 2 we use time-dependent variational principle (TDVP) for infinite matrix product states [59] to directly study the properties of the system in the thermodynamic limit. The power-law interactions in Eq. (1) were approximated as a sum of exponential functions and we used bond dimension $\chi = 128$ and time step $\delta t = 0.025$ (see Ref. [48] for further details).

We restrict to states with a two-site unit cell,

$$|\psi(0)\rangle = \bigotimes_i |+\rangle_{2i-1} (\cos\phi|+\rangle_{2i} + i \sin\phi|-\rangle_{2i}), \quad (3)$$

where $\phi = 0$ corresponds to spins polarized along the x-axis. The CTC order parameter is defined as $\langle\sigma^+\rangle \equiv (1/2)\sum_{i=1,2} |\langle\sigma_i^+\rangle|$, i.e., we average the *absolute* expectation value of $\sigma^+ \equiv (\sigma_x + i\sigma_y)/2$ over the sites in the unit cell. This is because, for our initial state, $\langle\sigma_{2i-1}^+\rangle = 1/2$ and $\langle\sigma_{2i}^+\rangle = \exp(-i2\phi)/2$, thus taking the absolute value allows us to detect the loss of magnetization due to U(1) symmetry breaking, rather than phase cancellations within the unit cell due to the choice of the initial state. We confirm that for $\alpha \lesssim 2.5$ the order parameter $\langle\sigma^+\rangle$ acquires a finite expectation value in the ground state of D. The local h_z field drives rotations in the x-y plane, causing the order parameter to oscillate periodically—the anticipated hallmark of the CTC phase. Figure 2 illustrates this by the dynamics of $D(t) \equiv \langle\psi(t)|D|\psi(t)\rangle$ (normalized by the value at $t = 0$), the von Neumann bipartite entanglement entropy $S_E(t)$ and the order parameter $\langle\sigma^+(t)\rangle$.

Figures 2(a)–2(c) are for the x-polarized ($\phi = 0$) initial state. As h_z is increased, the CTC phase is stabilized: D is well conserved, while $\langle\sigma^+(t)\rangle$ remains approximately

constant. For intermediate h_z, D does not decay to zero as typically seen in periodically driven systems [49]. This is due to the fact that h_z is a parameter in our Hamiltonian, rather than a driving frequency which pushes the system to infinite temperature. The fact that $\langle\sigma^+(t)\rangle$ remains approximately constant implies periodic oscillations in $\sigma_x(t)$ and $\sigma_y(t)$ with a period $T \approx 2\pi/h_z$. Because of the asymmetry between J_x and J_y couplings, $\langle\sigma^+(t)\rangle$ is not exactly conserved over time even in the prethermal phase, instead it oscillates between maxima (minima) when pointing along the x or y axis. This is also the cause of the small oscillations observed in D on the prethermal plateau. As our chosen initial state $|\psi(0)\rangle$ is close to the ground state of H_{eff} (but midspectrum for H), the growth of $S_E(t)$ is strongly suppressed for large h_z.

At high temperatures, the effective Hamiltonian transitions out of the CTC phase to a trivial disordered phase. The impact of energy density on the dynamics can be studied by varying ϕ in Eq. (3) to increase the energy density of the initial state. Dynamics for various choices of ϕ can be seen in Figs. 2(d)–2(f). These states are spread through the spectrum of H_{eff}, with $D(0)/N \approx \{-0.35, -0.26, -0.15 - 0.05, 0.05\}$, respectively. For all these states, D is well conserved, thus we remain in a prethermal phase. However, the increase in energy density means that the prethermal Gibbs state eventually becomes a high-temperature state and CTC order is lost. This is accompanied by $\langle\sigma^+(t)\rangle$ decaying to zero and faster growth of $S_E(t)$.

Many-body scars via "tunnels to towers."—Close to the isotropic point $J_x = J_y = J_z$, we find QMBS arise in the model (1) due to an approximate "tunnels-to-towers" mechanism [19]. The Z field term in the Hamiltonian in Eq. (1) possesses a spectrum generating algebra with respect to the raising operator of the standard SU(2) representation, $[Z, \sigma^+] = 2\sigma^+$. This trivially guarantees the eigenstates of Z form equidistant "towers." Taking Z, one can define a Hamiltonian by adding some additional term, specially chosen so as to preserve only a single tower of eigenstates of Z as eigenstates of the full Hamiltonian, while generically mixing other towers such that the resulting model is nonintegrable [19]. The preserved tower of eigenstates is found to be QMBS eigenstates. For example, they have subthermal entanglement entropy and coherent dynamics in all observables can be witnessed by preparing initial states with dominant support on the scarred subspace. Previous constructions of scarred Hamiltonians of this form have preserved a single tower of eigenstates exactly, in the sense that they remain exact eigenstates of the full Hamiltonian and therefore remain equidistant in energy. Sufficiently close to the isotropic point of the Hamiltonian in Eq. (1), these conditions are satisfied *approximately* (in [48] we quantify this). In this sense, a set of QMBS eigenstates are found in the spectrum of the Hamiltonian, which are approximately equidistant in energy and resemble some subset of exact eigenstates of Z. These QMBS eigenstates require weakly broken SU(2) symmetry and their presence is largely independent of α.

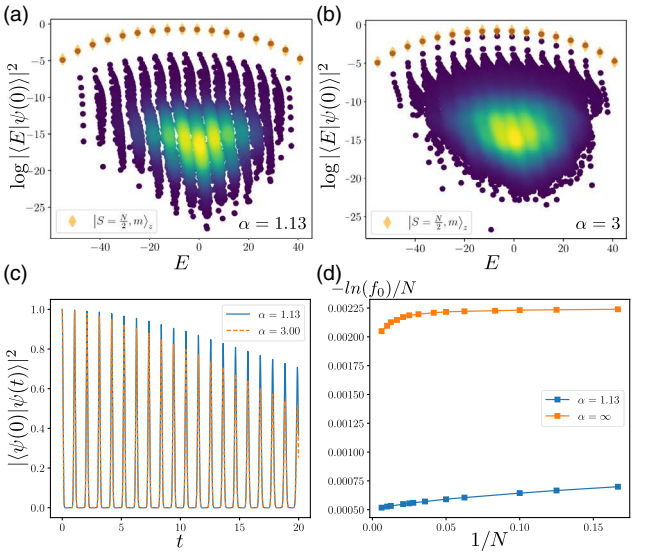

FIG. 3. Quantum many-body scars near the isotropic limit of the model in Eq. (1), with $J_x = -0.8$, $J_y = -1$, $J_z = -0.95$, $h_z = 3$ and system size $N = 16$. The initial state $|\psi(0)\rangle$ is x-polarized [$\phi = 0$ in Eq. (3)]. Top row: Eigenstate overlap with $|\psi(0)\rangle$ for both long-range (a) and short-range (b) models. In both cases, the top band of eigenstates are the QMBS eigenstates, which are well approximated by maximal-spin SU(2) basis states in the z-direction, denoted by diamonds. (c) Quantum fidelity revivals from the initial state $||\psi(0)\rangle$, for both long- and short-range models. (d) Finite-size scaling of the fidelity density $-\ln(f_0)/N$, where f_0 is the height of the first fidelity revival. The fidelity density, was obtained using finite TDVP with, bond dimension $\chi = 300$ and time step $\delta t = 0.02$.

In Fig. 3 we demonstrate the existence of QMBS eigenstates by exact diagonalization of a $N = 16$ site chain. We consider couplings close to the isotropic point, $J_x = -0.8$, $J_y = -1$, and $J_z = -0.95$. In Figs. 3(a) and 3(b) we plot the overlap of eigenstates with the x-polarized state [$\phi = 0$ in Eq. (3)], for both long-range ($\alpha = 1.13$) and short-range ($\alpha = 3$) models. In both cases, we see a top band of scarred eigenstates and note they resemble the large spin SU(2) basis states in the z-direction $|S = N/2, m\rangle$. These are precisely the eigenstates of Z which are approximately preserved as eigenstates of the full Hamiltonian. We note that in sectors with smaller total S, the towers of Z eigenstates no longer accurately describe the eigenstates of the full Hamiltonian (e.g., for the Néel state in the x-direction there are no visible towers). As the x-polarized state has dominant support on the QMBS eigenstates which are approximately equidistant in energy, it follows that initializing the system in this state results in a periodic trajectory in the Hilbert space, demonstrated by the revivals in quantum fidelity, $f(t) = |\langle\psi(0)|\psi(t)\rangle|^2$, in Fig. 3(c). We confirm that the nonergodic dynamics from such initial

states persists in the thermodynamic limit by performing finite-size scaling of the fidelity density $-\ln(f_0)/N$, where f_0 is the amplitude of the first fidelity revival. The fidelity density in Fig. 3(d) converges to a value much smaller than ln(2), expected for a random initial state in a thermalizing system. The extrapolated value is of the same order for both long- and short-range models, indicating the persistence of ergodicity breaking due to QMBS.

Conclusions.—We demonstrated that a long-range interacting XYZ spin model in a magnetic field realizes two types of weak ergodicity breaking phenomena—a CTC phase and QMBS states—allowing us to controllably tune between them by varying the interaction anisotropies. While generally distinct phenomena, QMBS and CTC coexist when both $J_{\mathrm{U}(1)}$ and $J_{\mathrm{SU}(2)}$ are small, as indicated in Fig. 1, raising interesting questions about their distinguishability in that regime. A possible intertwining of QMBS with discrete, rather than continuous, time crystal was explored in recent works [12,60], which studied QMBS in the presence of external periodic driving. It was found that when the drive period is approximately half of the QMBS revival time, the QMBS can be stabilized, while avoiding thermalization due to the same principles that suppress thermalization in our case for large h_z. The interplay is subtle: the ideal drive pulses lead to a complete cancellation of the Floquet Hamiltonian, such that *all* initial states revive [60]. Imperfect driving leads to nontrivial dynamics, which—surprisingly—tends to better preserve some QMBS than generic states. There is a very rich phenomenology that is being uncovered in this setting but many questions regarding the stabilization mechanism and sensitivity to the initial state remain open [61,62].

Our results on the undriven XYZ model suggest that CTC and QMBS can be distinguished by the quench dynamics from different initial states. QMBS occur for initial states that have a large overlap with the large-S spin sector (such as the x-polarized state), regardless of energy density. The lifetime of the scarring revivals is exponentially sensitive to $J_{\mathrm{SU}(2)}$. Moreover, QMBS place stronger constraints on the dynamics, leading to the wave function fidelity revivals, in addition to the oscillations of a local order parameter. In contrast, the CTC manifests for initial states that have low energy density with respect to D, but not necessarily large support on a large-S spin sector. Hence, CTC is expected to persist for other initial states, such as the two-site unit cell states in Eq. (3), as long as those are below the critical energy density with respect to D. The CTC oscillations depend weakly on $J_{\mathrm{SU}(2)}$ but their lifetime is exponentially long in $h_z/J_{\mathrm{U}(1)}$. In future work, it would be interesting to analyze the behavior of CTC for initial states beyond period 2, e.g., the spiral states recently used in Ref. [63], as well as possible realizations of CTC and QMBS in local models in higher dimensions.

In compliance with EPSRC policy framework on research data, this publication is theoretical work that does not require supporting research data.

We thank Alessio Lerose and Bela Bauer for useful discussions. K. B., A. H., and Z. P. acknowledge support by EPSRC Grants No. EP/R020612/1 and No. EP/M50807X/1, and by the Leverhulme Trust Research Leadership Award No. RL-2019-015. I. M. was supported by the U.S. Department of Energy, Office of Science, Basic Energy Sciences, Materials Sciences and Engineering Division.

[1] Hannes Bernien, Sylvain Schwartz, Alexander Keesling, Harry Levine, Ahmed Omran, Hannes Pichler, Soonwon Choi, Alexander S. Zibrov, Manuel Endres, Markus Greiner, Vladan Vuletić, and Mikhail D. Lukin, Probing many-body dynamics on a 51-atom quantum simulator, Nature (London) **551**, 579 (2017).

[2] Maksym Serbyn, Dmitry A Abanin, and Zlatko Papić, Quantum many-body scars and weak breaking of ergodicity, Nat. Phys. **17**, 675 (2021).

[3] Sanjay Moudgalya, B. Andrei Bernevig, and Nicolas Regnault, Quantum many-body scars and Hilbert space fragmentation: A review of exact results, Rep. Prog. Phys. **85**, 086501 (2022).

[4] C. J. Turner, A. A. Michailidis, D. A. Abanin, M. Serbyn, and Z. Papić, Weak ergodicity breaking from quantum many-body scars, Nat. Phys. **14**, 745 (2018).

[5] Wen Wei Ho, Soonwon Choi, Hannes Pichler, and Mikhail D. Lukin, Periodic Orbits, Entanglement, and Quantum Many-Body Scars in Constrained Models: Matrix Product State Approach, Phys. Rev. Lett. **122**, 040603 (2019).

[6] Soonwon Choi, Christopher J. Turner, Hannes Pichler, Wen Wei Ho, Alexios A. Michailidis, Zlatko Papić, Maksym Serbyn, Mikhail D. Lukin, and Dmitry A. Abanin, Emergent SU(2) Dynamics and Perfect Quantum Many-Body Scars, Phys. Rev. Lett. **122**, 220603 (2019).

[7] Kieran Bull, Jean-Yves Desaules, and Zlatko Papić, Quantum scars as embeddings of weakly broken Lie algebra representations, Phys. Rev. B **101**, 165139 (2020).

[8] Christopher J. Turner, Jean-Yves Desaules, Kieran Bull, and Zlatko Papić, Correspondence Principle for Many-Body Scars in Ultracold Rydberg Atoms, Phys. Rev. X **11**, 021021 (2021).

[9] Eric J. Heller, Bound-State Eigenfunctions of Classically Chaotic Hamiltonian Systems: Scars of Periodic Orbits, Phys. Rev. Lett. **53**, 1515 (1984).

[10] A. A. Michailidis, C. J. Turner, Z. Papić, D. A. Abanin, and M. Serbyn, Stabilizing two-dimensional quantum scars by deformation and synchronization, Phys. Rev. Research **2**, 022065(R) (2020).

[11] Cheng-Ju Lin, Vladimir Calvera, and Timothy H. Hsieh, Quantum many-body scar states in two-dimensional Rydberg atom arrays, Phys. Rev. B **101**, 220304(R) (2020).

[12] D. Bluvstein, A. Omran, H. Levine, A. Keesling, G. Semeghini, S. Ebadi, T. T. Wang, A. A. Michailidis, N. Maskara, W. W. Ho, S. Choi, M. Serbyn, M. Greiner,

V. Vuletić, and M. D. Lukin, Controlling quantum many-body dynamics in driven Rydberg atom arrays, Science **371**, 1355 (2021).
[13] C. J. Turner, A. A. Michailidis, D. A. Abanin, M. Serbyn, and Z. Papić, Quantum scarred eigenstates in a Rydberg atom chain: Entanglement, breakdown of thermalization, and stability to perturbations, Phys. Rev. B **98**, 155134 (2018).
[14] Vedika Khemani, C. R. Laumann, and Anushya Chandran, Signatures of integrability in the dynamics of Rydberg-blockaded chains, Phys. Rev. B **99**, 161101(R) (2019).
[15] Cheng-Ju Lin, Anushya Chandran, and Olexei I. Motrunich, Slow thermalization of exact quantum many-body scar states under perturbations, Phys. Rev. Research **2**, 033044 (2020).
[16] Ian Mondragon-Shem, Maxim G. Vavilov, and Ivar Martin, Fate of quantum many-body scars in the presence of disorder, PRX Quantum **2**, 030349 (2021).
[17] Sanjay Moudgalya, Nicolas Regnault, and B. A. Bernevig, Entanglement of exact excited states of Affleck-Kennedy-Lieb-Tasaki models: Exact results, many-body scars, and violation of the strong eigenstate thermalization hypothesis, Phys. Rev. B **98**, 235156 (2018).
[18] Daniel K. Mark, Cheng-Ju Lin, and Olexei I. Motrunich, Unified structure for exact towers of scar states in the Affleck-Kennedy-Lieb-Tasaki and other models, Phys. Rev. B **101**, 195131 (2020).
[19] Nicholas O'Dea, Fiona Burnell, Anushya Chandran, and Vedika Khemani, From tunnels to towers: Quantum scars from Lie algebras and q-deformed Lie algebras, Phys. Rev. Research **2**, 043305 (2020).
[20] Naoto Shiraishi and Takashi Mori, Systematic Construction of Counterexamples to the Eigenstate Thermalization Hypothesis, Phys. Rev. Lett. **119**, 030601 (2017).
[21] Michael Schecter and Thomas Iadecola, Weak Ergodicity Breaking and Quantum Many-Body Scars in Spin-1 XY Magnets, Phys. Rev. Lett. **123**, 147201 (2019).
[22] Berislav Buča, Joseph Tindall, and Dieter Jaksch, Non-stationary coherent quantum many-body dynamics through dissipation, Nat. Commun. **10**, 1730 (2019).
[23] Kieran Bull, Ivar Martin, and Z. Papić, Systematic Construction of Scarred Many-Body Dynamics in 1D Lattice Models, Phys. Rev. Lett. **123**, 030601 (2019).
[24] Naoyuki Shibata, Nobuyuki Yoshioka, and Hosho Katsura, Onsager's Scars in Disordered Spin Chains, Phys. Rev. Lett. **124**, 180604 (2020).
[25] Sanjay Moudgalya, Edward O'Brien, B. A. Bernevig, Paul Fendley, and Nicolas Regnault, Large classes of quantum scarred Hamiltonians from matrix product states, Phys. Rev. B **102**, 085120 (2020).
[26] K. Pakrouski, P. N. Pallegar, F. K. Popov, and I. R. Klebanov, Many-Body Scars as a Group Invariant Sector of Hilbert Space, Phys. Rev. Lett. **125**, 230602 (2020).
[27] Jie Ren, Chenguang Liang, and Chen Fang, Quasisymmetry Groups and Many-Body Scar Dynamics, Phys. Rev. Lett. **126**, 120604 (2021).
[28] Federica Maria Surace, Giuliano Giudici, and Marcello Dalmonte, Weak-ergodicity-breaking via lattice supersymmetry, Quantum **4**, 339 (2020).
[29] Yoshihito Kuno, Tomonari Mizoguchi, and Yasuhiro Hatsugai, Flat band quantum scar, Phys. Rev. B **102**, 241115(R) (2020).
[30] J. M. Deutsch, Quantum statistical mechanics in a closed system, Phys. Rev. A **43**, 2046 (1991).
[31] Mark Srednicki, Chaos and quantum thermalization, Phys. Rev. E **50**, 888 (1994).
[32] Dominic V. Else, Bela Bauer, and Chetan Nayak, Prethermal Phases of Matter Protected by Time-Translation Symmetry, Phys. Rev. X **7**, 011026 (2017).
[33] Dmitry Abanin, Wojciech De Roeck, Wen Wei Ho, and François Huveneers, A rigorous theory of many-body prethermalization for periodically driven and closed quantum systems, Commun. Math. Phys. **354**, 809 (2017).
[34] Soonwon Choi, Joonhee Choi, Renate Landig, Georg Kucsko, Hengyun Zhou, Junichi Isoya, Fedor Jelezko, Shinobu Onoda, Hitoshi Sumiya, Vedika Khemani, Curt von Keyserlingk, Norman Y. Yao, Eugene Demler, and Mikhail D. Lukin, Observation of discrete time-crystalline order in a disordered dipolar many-body system, Nature (London) **543**, 221 (2017).
[35] J. Zhang, P. W. Hess, A. Kyprianidis, P. Becker, A. Lee, J. Smith, G. Pagano, I.-D. Potirniche, A. C. Potter, A. Vishwanath, N. Y. Yao, and C. Monroe, Observation of a discrete time crystal, Nature (London) **543**, 217 (2017).
[36] J. Randall, C. E. Bradley, F. V. van der Gronden, A. Galicia, M. H. Abobeih, M. Markham, D. J. Twitchen, F. Machado, N. Y. Yao, and T. H. Taminiau, Many-body localized discrete time crystal with a programmable spin-based quantum simulator, Science **374**, 1474 (2021).
[37] Xiao Mi *et al.*, Time-crystalline eigenstate order on a quantum processor, Nature (London) **601**, 531 (2022).
[38] A. Kyprianidis, F. Machado, W. Morong, P. Becker, K. S. Collins, D. V. Else, L. Feng, P. W. Hess, C. Nayak, G. Pagano, N. Y. Yao, and C. Monroe, Observation of a prethermal discrete time crystal, Science **372**, 1192 (2021).
[39] William Beatrez, Christoph Fleckenstein, Arjun Pillai, Erica Sanchez, Amala Akkiraju, Jesus Alcala, Sophie Conti, Paul Reshetikhin, Emanuel Druga, Marin Bukov, and Ashok Ajoy, Observation of a long-lived prethermal discrete time crystal created by two-frequency driving, arXiv:2201.02162.
[40] Vedika Khemani, Achilleas Lazarides, Roderich Moessner, and S. L. Sondhi, Phase Structure of Driven Quantum Systems, Phys. Rev. Lett. **116**, 250401 (2016).
[41] Dominic V. Else, Bela Bauer, and Chetan Nayak, Floquet Time Crystals, Phys. Rev. Lett. **117**, 090402 (2016).
[42] C. W. von Keyserlingk, Vedika Khemani, and S. L. Sondhi, Absolute stability and spatiotemporal long-range order in Floquet systems, Phys. Rev. B **94**, 085112 (2016).
[43] N. Y. Yao, A. C. Potter, I.-D. Potirniche, and A. Vishwanath, Discrete Time Crystals: Rigidity, Criticality, and Realizations, Phys. Rev. Lett. **118**, 030401 (2017).
[44] Wen Wei Ho, Soonwon Choi, Mikhail D. Lukin, and Dmitry A. Abanin, Critical Time Crystals in Dipolar Systems, Phys. Rev. Lett. **119**, 010602 (2017).
[45] Krzysztof Sacha and Jakub Zakrzewski, Time crystals: A review, Rep. Prog. Phys. **81**, 016401 (2018).

[46] Vedika Khemani, Roderich Moessner, and S. L. Sondhi, A brief history of time crystals (2019).
[47] Dominic V. Else, Christopher Monroe, Chetan Nayak, and Norman Y. Yao, Discrete time crystals, arXiv:1905.13232.
[48] See Supplemental Material at http://link.aps.org/supplemental/10.1103/PhysRevLett.129.140602 for details of the analytic and numerical studies of the phase diagram.
[49] Francisco Machado, Dominic V. Else, Gregory D. Kahanamoku-Meyer, Chetan Nayak, and Norman Y. Yao, Long-Range Prethermal Phases of Nonequilibrium Matter, Phys. Rev. X **10**, 011043 (2020).
[50] Mohammad F. Maghrebi, Zhe-Xuan Gong, and Alexey V. Gorshkov, Continuous Symmetry Breaking in 1D Long-Range Interacting Quantum Systems, Phys. Rev. Lett. **119**, 023001 (2017).
[51] H. J. Lipkin, N. Meshkov, and A. J. Glick, Validity of many-body approximation methods for a solvable model: (i). exact solutions and perturbation theory, Nucl. Phys. **62**, 188 (1965).
[52] N. Meshkov, A. J. Glick, and H. J. Lipkin, Validity of many-body approximation methods for a solvable model: (ii). linearization procedures, Nucl. Phys. **62**, 199 (1965).
[53] Bruno Sciolla and Giulio Biroli, Quantum Quenches and Off-Equilibrium Dynamical Transition in the Infinite-Dimensional Bose-Hubbard Model, Phys. Rev. Lett. **105**, 220401 (2010).
[54] Bruno Sciolla and Giulio Biroli, Quantum quenches, dynamical transitions, and off-equilibrium quantum criticality, Phys. Rev. B **88**, 201110(R) (2013).
[55] Alessio Lerose and Silvia Pappalardi, Bridging entanglement dynamics and chaos in semiclassical systems, Phys. Rev. A **102**, 032404 (2020).
[56] Takashi Mori, Prethermalization in the transverse-field Ising chain with long-range interactions, J. Phys. A **52**, 054001 (2019).
[57] P. W. Anderson, An approximate quantum theory of the antiferromagnetic ground state, Phys. Rev. **86**, 694 (1952).
[58] Hal Tasaki, Long-range order, "tower" of states, and symmetry breaking in lattice quantum systems, J. Stat. Phys. **174**, 735 (2019).
[59] Jutho Haegeman, J. Ignacio Cirac, Tobias J. Osborne, Iztok Pižorn, Henri Verschelde, and Frank Verstraete, Time-Dependent Variational Principle for Quantum Lattices, Phys. Rev. Lett. **107**, 070601 (2011).
[60] N. Maskara, A. A. Michailidis, W. W. Ho, D. Bluvstein, S. Choi, M. D. Lukin, and M. Serbyn, Discrete Time-Crystalline Order Enabled by Quantum Many-Body Scars: Entanglement Steering via Periodic Driving, Phys. Rev. Lett. **127**, 090602 (2021).
[61] Guo-Xian Su, Hui Sun, Ana Hudomal, Jean-Yves Desaules, Zhao-Yu Zhou, Bing Yang, Jad C. Halimeh, Zhen-Sheng Yuan, Zlatko Papić, and Jian-Wei Pan, Observation of unconventional many-body scarring in a quantum simulator, arXiv:2201.00821.
[62] Ana Hudomal, Jean-Yves Desaules, Bhaskar Mukherjee, Guo-Xian Su, Jad C. Halimeh, and Zlatko Papić, Driving quantum many-body scars, Phys. Rev. B **106**, 104302 (2022).
[63] P. N. Jepsen, Y. K. Lee, H. Lin, I. Dimitrova, Y. Margalit, W. W. Ho, and W. Ketterle, Long-lived phantom helix states in Heisenberg quantum magnets Nat. Phys. 18, 899 (2022).